Self-learning Voxel-based Multi-camera Occlusion Maps for 3D Reconstruction

Maarten Slembrouck[1], Dimitri Van Cauwelaert[1], David Van Hamme[1], Dirk Van Haerenborgh[1], Peter Van Hese[1], Peter Veelaert[1] and Wilfried Philips[1 2]

[1]*Ghent University, TELIN dept. IPI/iMinds, Ghent, Belgium*

[2]*Senior member of IEEE*

maarten.slembrouck@ugent.be

Keywords: Multi-camera, Occlusion Detection, Self-learning, Visual hull

Abstract: The quality of a shape-from-silhouettes 3D reconstruction technique strongly depends on the completeness of the silhouettes from each of the cameras. Static occlusion, due to e.g. furniture, makes reconstruction difficult, as we assume no prior knowledge concerning shape and size of occluding objects in the scene. In this paper we present a self-learning algorithm that is able to build an occlusion map for each camera from a voxel perspective. This information is then used to determine which cameras need to be evaluated when reconstructing the 3D model at every voxel in the scene. We show promising results in a multi-camera setup with seven cameras where the object is significantly better reconstructed compared to the state of the art methods, despite the occluding object in the center of the room.

1 INTRODUCTION

Occlusion is undesirable for computer vision applications such as 3D reconstruction based on shape-from-silhouettes [Laurentini, 1994, Corazza et al., 2006, Corazza et al., 2010, Grauman et al., 2003] because parts of the object disappear in the foreground-background segmentation. However, in real-world applications occlusion is unavoidable. In order to handle occlusion, we propose a self-learning algorithm that determines occlusion for every voxel in the scene. We focus on occlusion as a result of static objects between the object and the camera.
Algorithms to detect partial occlusion are presented in [Guan et al., 2006, Favaro et al., 2003, Apostoloff and Fitzgibbon, 2005, Brostow and Essa, 1999]. However, in these papers occlusion is detected from the camera view itself by keeping an occlusion map which is a binary decision for each of its pixels. An OR-operation between the foreground/background mask and the occlusion mask, results in the input masks for the visual hull algorithm. The major drawback to this approach is that occlusion is in fact voxel-related, rather than pixel-related: the same pixel in an image is occluded when the occluding object is located between the object and the camera, but not if the object is placed between the camera and the occluding object. Pixel-based occlusion detection results in a 3D model which consists of far more voxels not belonging to the 3D model because the occluder is also reconstructed and depending on the position of the person, parts of the occluder are still left over after subtracting the visual hull of the occluder (we will show this in Section 5).

Therefore, we propose an occlusion map (one for each camera) from a voxel perspective, in order to evaluate each voxel separately. After the occlusion maps are built, we can use this information and only evaluate the camera views which are not occluded and therefore contribute to the 3D model.

We determine occlusion and non-occlusion based on a fast algorithm of the visual hull concept. In order for the system to work, the occlusion algorithm requires someone walking in the scene to make occluded regions appear. Subsets of the different camera views are used to increase the votes for either occlusion or non-occlusion for each voxel. A majority vote decides about the final classification.

We also assign a quality factor to the subset of chosen cameras because the volume of the visual hull strongly depends on the camera positions. Instead of counting integer votes, we increment by the quality factor which depends both on the combined cameras

This research was made possible through iMinds, an independent research institute founded by the Flemish government.

and the voxel position.
In Section 2 we explain the fast visual hull algorithm. Section 3 proposes the self-learning occlusion algorithm. We determine the quality factor for a camera combination which is used for voting in Section 4. In Section 5 we show the promising results of our test setup.

2 FAST VISUAL HULL COMPUTATION

The visual hull of an object is determined by its silhouettes as a result of the foreground-background segmentation [Kim et al., 2006, Zivkovic, 2004] and the intrinsically and extrinsically camera calibration parameters. We use a voxel representation for the visual hull to reduce computation time. It is required that all cameras face the same area, called the overlapping area, because that is the only area where a 3D model can be built using all cameras with this implementation.

2.1 Fast visual hull algorithm

Our fast visual hull algorithm loops over all voxels in a bounded area. For each voxel, the foreground masks are evaluated at its projected image coordinates for each camera. A voxel is part of the visual hull, only if all projections are classified as foreground. Algorithm 1 shows our fast visual hull implementation.

Algorithm 1 Fast visual hull algorithm

```
input: camera calibration, FG/BG-masks, bounded area

output: voxelated visual hull

for all voxel in voxel_space do
   while voxel occupied and not all camera views evaluated do
      lookup the voxel's projection on next camera view
      if projection is foreground then
         classify voxel as occupied
      else
         classify voxel as unoccupied
      end if
   end while
end for
```

2.2 Optimization

Within a particular multi-camera setup, the projections of the voxels are always the same as long as the cameras do not move. Therefore, we calculate the image coordinates corresponding to each voxel center in the scene in the precomputation phase of our visual hull algorithm and use a lookup table to determine the image coordinates. Equation 1 shows how the voxel center (X,Y,Z) is projected onto the image sensor, resulting in pixel coordinates (x,y). The projection matrix P is the product of the intrinsic camera matrix and the transformation matrix $(R|T)$.

$$\begin{pmatrix} x \\ y \\ 1 \end{pmatrix} = \overbrace{\begin{pmatrix} f_x & 0 & c_x \\ 0 & f_y & c_y \\ 0 & 0 & 1 \end{pmatrix} \begin{pmatrix} r_{11} & r_{12} & r_{13} & t_1 \\ r_{21} & r_{22} & r_{23} & t_2 \\ r_{31} & r_{32} & r_{33} & t_3 \end{pmatrix}}^{P} \begin{pmatrix} X \\ Y \\ Z \\ 1 \end{pmatrix} \quad (1)$$

Note that this does not lead to an exact reconstruction because only the center of each voxel is evaluated making it suitable for solid objects but not for objects with holes. For each camera the traditional implementation projects eight points (voxel corners) and evaluates all pixels within their convex hull whereas we only project a single point (voxel center) and evaluate this pixel value. The major advantage of our approach is that it increases the speed significantly (more than 8 times faster).

3 SELF-LEARNING OCCLUSION ALGORITHM

Visual hull algorithms are inherently sensitive to misclassified pixels in the foreground-background segmentation, the presence of which is to be expected when camera views are occluded by one or more objects. Therefore we propose a self-learning algorithm which determines for every voxel if it is occluded for any of the cameras. Hence, the number of occlusion maps equals the number of cameras in the room.

3.1 Deciding if a voxel is occluded

Deciding whether a voxel is occluded or not does not seem to be an easy task. In previous research, occlusion was determined from pixel perspective but this is not sufficient because of the following reason. Consider a piece of furniture in the middle of the scene (e.g. a closet). From the perspective of a particular camera, a person can stand in front of the furniture or behind it, resulting in occlusion by the closet in the latter case. But if we look at the occluding pixels from the camera view, we see the pixels are only occluded when the person stands behind the closet. When the person stands in front of it, those same pixels should not be considered as occluded pixels because they hold relevant information. Since standard cameras do not have depth information it is not sufficient to keep track of occluded pixels, therefore we use occluded voxels.

To decide if there is occlusion, we make some assumptions. One of these assumptions is that there needs to be a consensus about the occupation of a voxel in the space. This consensus is only possible if a minimum number of cameras agree that a voxel at a certain place in space is occupied. If there are for example three cameras agreeing there is an object at a certain position in space, but the fourth camera does not detect anything there, then we can quite safely assume that those unseen voxels are occluded for the fourth camera. However, it is not clear how many cameras need to agree about this visibility. One could expect as much as possible, but this will fail if there is a lot of occlusion because the consensus will be lacking.

Since it is hard to decide whether a voxel is occluded for a certain camera, we count votes for both cases: *occluded* and *non-occluded*. Every voxel has a separate count for each camera for both classes. The only requirement is that a person needs to walk around in the scene to make occluded regions appear. Voxels outside the field of view of the cameras are directly classified as occluded because these voxels are out of sight. In the following sections we explain our detection mechanism for both occlusion and non-occlusion in detail.

3.1.1 Visible

Figure 1 shows a flowchart explaining how we determine the absence of occlusion for camera C_0. Basically, we randomly pick two other cameras and generate the visual hull from the masks of camera C_0 and these two cameras C_a and C_b. The voxels defining this visual hull are the ones who are not occluded for all these cameras, otherwise they should be carved out of the visual hull.

3.1.2 Occluded

One could think that no absence of occlusion means occlusion but that would be wrong because we can only determine occlusion in the zone where the person is walking and it strongly depends on the chosen cameras. Determining occlusion is much more complicated. Figure 2 shows the flowchart to understand the algorithm. We first generate the visual hull with only the camera of which we want to determine occlusion, camera C_0. We randomly pick three cameras and reproject the generalized cone of C_0 back on each of the camera image planes of these cameras: C_a, C_b and C_c. This reprojection results in a different mask for each camera $mask_{repr,C_x}$ with $x = a$, b or c.

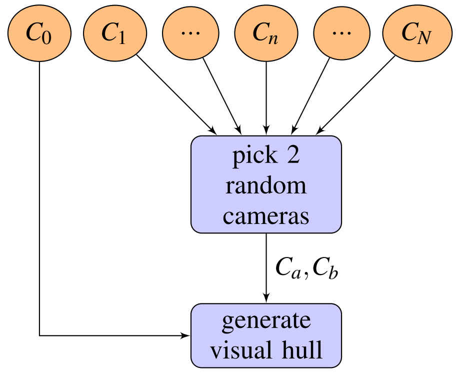

Figure 1: Flowchart to determine which voxels are not occluded for camera C_0. Two cameras are randomly picked from the list and we calculate the visual hull from their masks together with the mask of camera C_0 from which we try to determine the occlusion map. Since camera C_0 contributes to the visual hull the result is a shape which is not occluded for these cameras.

An example is shown in Figure 3. In Figure 3a we see the mask of camera C_0. If we look closely we see that only half of the person is visible in this mask which means there is occlusion. Figure 3b shows the mask from another camera ($mask_{fgbg,C_a}$) which sees the entire person. We compare $mask_{fgbg,C_a}$ with $mask_{repr,C_a}$ (Figure 3c), which is the reprojected visual hull from camera C_0 onto this other camera, according to (FG = foreground and BG = background):

$$mask_{occl,C_x}(x,y) = mask_{repr,C_a}(x,y) = BG \wedge mask_{fgbg,C_x}(x,y) = FG \quad (2)$$

The result ($mask_{occl,C_a}$) is shown in Figure 3d which indicates the invisible parts for camera C_0 in white. The same calculations are made for the two other randomly chosen cameras. These three masks, in respect to the correct camera viewpoints, produce a visual hull which consists mostly of occluded voxels for camera C_0. Due to the visual hull algorithm, we cannot guarantee that all of its voxels are really occluded, hence the voting framework.

Notice that the self-learning occlusion algorithm also solves another problem. Namely, when the foreground-background segmentation continuously fails to classify certain pixels as foreground, the votes for occlusion will increase and the system will eventually ignore that camera for those pixels which offers a great advantage since it would otherwise degrade the 3D model as well.

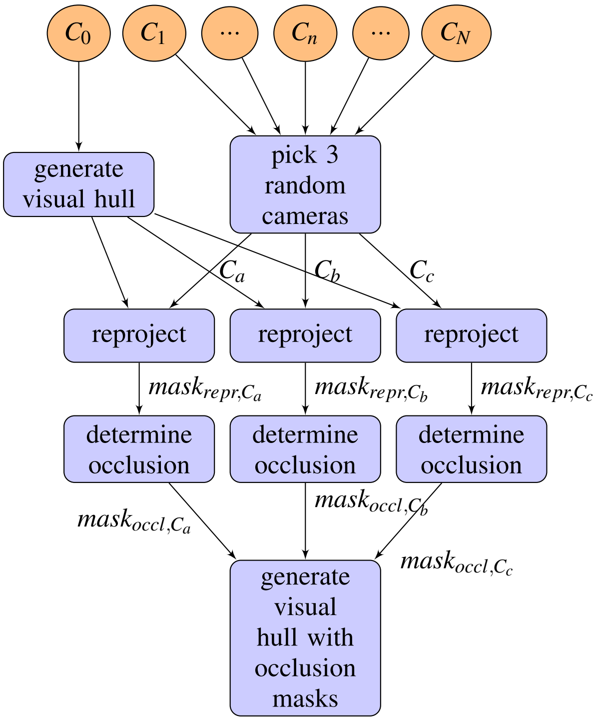

Figure 2: Flowchart to determine occlusion for camera C_0. First we pick three random cameras from the list ($C_1 - C_N$) and also calculate the visual hull for C_0 only (in a bounded area). Next, we reproject that visual hull on each of the sensors of the chosen cameras. We then compare this reprojected mask with the original mask of the respective camera (using formula 2). This results in occlusion masks for the three randomly picked cameras. The visual hull generated by these occlusion masks determines the occluded voxels for camera C_0 in that time frame. In case of static occlusion the complete occlusion map will be built over time.

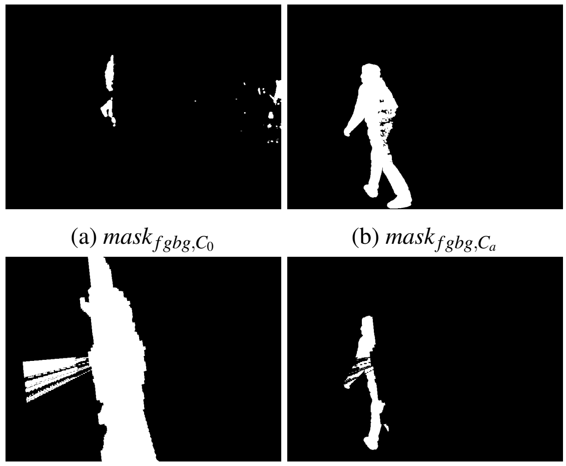

(a) $mask_{fgbg,C_0}$ (b) $mask_{fgbg,C_a}$

(c) $mask_{repr,C_a}$ (d) $mask_{occl,C_a}$

Figure 3: (a) The mask of the camera C_0 for which occlusion is checked. (b) The mask of one of the randomly chosen camera views C_a (c). The reprojected image of the visual hull generated only by mask (a). (d) The occluded part shown in white, which is combined with two other cameras to calculate a visual hull and update the occlusion map.

4 QUALITY FACTOR VOTING

In a multi-camera setup not all cameras are equally relevant to a certain voxel in space. Not only the distance to the camera, but also the angles between the cameras (with the voxel as center) determine the relevance of the information added by each camera. The self-learning occlusion algorithm takes this into account: we add this relevance as a quality factor to the framework. Rather than counting the number of votes, we count these quality factors Q ($0 \leq Q \leq 1$). The count for both cases, t_{occluded} and t_{visible} are kept:

$$\begin{aligned} t_{\text{occluded}} &= t_{\text{occluded}} + Q \\ t_{\text{visible}} &= t_{\text{visible}} + Q \end{aligned} \tag{3}$$

The visual hull provides a qualitative tool for measuring the relevance of a camera. For every camera we add to the scene, the resulting 3D model is composed by the same or less voxels, since every new camera carves away zero or more voxels. In the next section we investigate the influence of angle differences between given cameras with respect to the resulting visual hull.

4.1 Quality factor for two cameras

We first consider the two-dimensional problem. In case of two cameras we can visualize the influence of the angle variation by keeping both cameras at the same distance of the object. Because the overlapping area equals infinity for small angles, we decided to restrict the overlapping space in a well defined circular area. Figure 4 shows three different angles: 20°, 90° and 180°. For an aperture angle of 20° they result in a visual hull of 2.99%, 0.75% and 4.08% respectively of the space described by the circle through C1 and C2, and the voxel as its center. In Figure 5 we see the overlapping area as a function of the angle (range from 0° till 180°.
We distinguish three different zones: $0-20°$, $20-160°$ and $160-180°$. In the first part, the overlapping area is equal to infinity because the overlapping area is not bounded, both cameras are looking in the same direction from the same position. In the second part, we find a more or less symmetrical course with 90° corresponding to the minimum overlapping area. The third part results in a constant overlapping area because both cameras are then facing each other. The quality factors need to show the same trend.

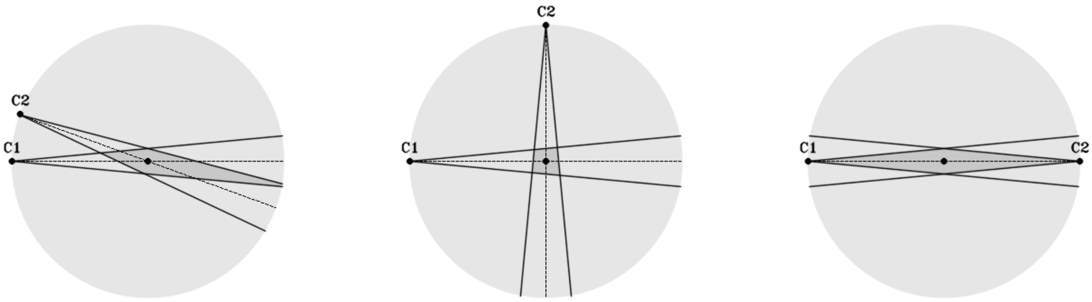

(a) (b) (c)

Figure 4: Overlapping area for an angle of 20°, 90° and 180° between camera C1 and C2 for a certain voxel in space. We see that the overlapping area (dark gray area) presents respectively 2.99%, 0.75% and 4.08% of the marked space (lightgray area). We notice an angle of 90° reduces the overlapping area significantly.

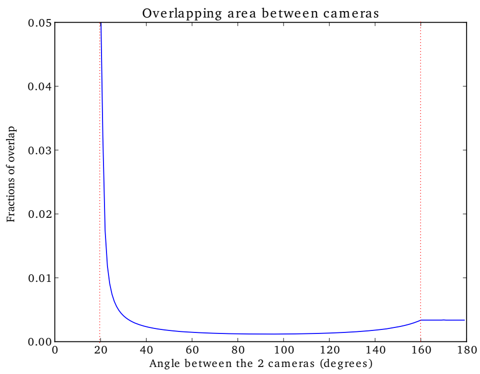

Figure 5: The fraction of overlap between views of two cameras equidistant from a certain voxel, both having a viewing angle of 20°, as a function of the angle between the cameras. The graph between 180° and 360° is a horizontally mirrored version of this first part.

4.2 Proposed quality calculation for multiple cameras

In case of more cameras, we determine the quality factor of the chosen cameras with a practical approach. Since we have a fully calibrated camera setup, we are able to determine the visual hull of virtual objects with a number of cameras in this space and because we know the virtual object, we are able to compare the volume of the visual hull with the volume of the original object. Because voxels are cubes, we opted for this shape. Each cube has the center of a voxel as its own center. In order to reconstruct the cube, the corners of the cubes are projected on each of the image planes (equation **??**). The convex hull of these image coordinates represents the projection of the virtual cube on the image plane. Consequently, the visual hull of the cube is build from these projections.

From the previous section we know that the volume of the visual hull V_{VH} strongly depends on position of the cameras, hence we use V_{VH} to calculate the quality factor Q. The combination of cameras that has the smallest visual hull needs to be granted the highest quality. Therefore we calculate the ratio of the volume of the original cube V_{cube} and the volume of this visual hull V_{VH} and use this as quality factor Q (equation 4).

$$Q = \frac{V_{cube}}{V_{VH}} \tag{4}$$

From the properties of a visual hull, we know that $V_{VH} \geq V_{cube}$. Therefore Q always satisfies $0 \leq Q \leq 1$. The most accurate results are obtained by using the voxels as cubes to calculate the visual hull. However, in that case, we need subvoxel precision, which would increase the memory usage significantly. Therefore, we chose to use the same voxel resolution (2 cm^3) as the voxel resolution we use for the visual hull algorithm and we use cubes with edges equal to a multiple of the voxel resolution (e.g. 20 cm^3).

In the pre-computation phase we calculate the quality factors for all possible combinations of three cameras. In case of seven cameras, that means $\binom{7}{3} = 35$ unique combinations for every voxel. To reduce computation time we opt to calculate the aforementioned quality factors for an oversampled voxel space (every 10cm in each direction). The quality factors of the intermediary voxels are calculated from its eight nearest neighbours in this oversampled voxel space using weighted averaging (Figure 7). Equation 5 calculates this weighted average. We define $P_{cube,i}$ as one of the eight nearest corners from the oversampled voxel space. The weights are equal to the euclidean distance between such a corner point $P_{cube,i}$ and the point P we want to calculate the interpolated quality factor for. Q_i represents the quality factor of the voxel at $P_{cube,i}$.

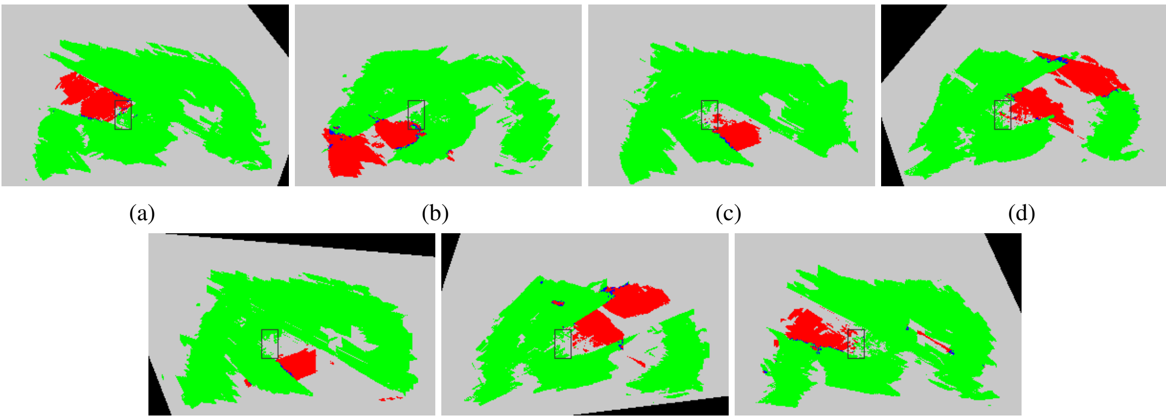

(a) (b) (c) (d)

(e) (f) (g)

Figure 6: One horizontal layer (1.20 m above ground level) of the occlusion maps of all cameras. (a) bottom right corner, (b) upper right corner, (c) upper left corner, (d) lower left corner, (e) upper left corner, (f) lower left corner and (g) lower right corner. The top row shows the occlusion maps from cameras at 3.5 m from the ground, the bottom row from the cameras 1.2 m from the ground. The black rectangle represents the occlusion object. We distinguish five classes: occluded (red), non-occluded (green), undecided (blue), unknown (gray) and out of sight (black). Errors in the occlusion map are due to noise in the foreground-background images.

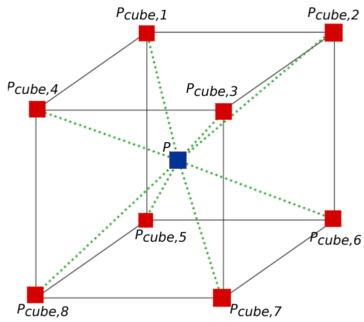

Figure 7: Interpolation of intermediary voxels. Red filled squares represent voxels from the oversampled voxel space while the blue squares inside the cube represents a voxel from the normal voxel space. Green dashed lines represent the distance from the center of the voxel P to one of the cube corner voxels.

$$Q_P = \frac{\sum_{i=1}^{8} d(P_{cube,i}, P) Q_i}{\sum_{i=1}^{8} d(P_{cube,i}, P)} \tag{5}$$

5 RESULTS

5.1 Test setup

We made a test setup of 8m×4m×3.5m ($w \times l \times h$) with seven cameras, four of them placed in the top four corners and three others about 1.2 m from the ground on the vertical edges. In the middle of the room we placed an occluding object (Figure 8). All cameras have 780×580 px image resolution. We calibrated all cameras intrinsically and extrinsically. In the next phase we asked a person to walk through the room. The aim is to visit each voxel near occluding objects at least once. However, the more often the person visits a certain voxel, the more certain the system becomes about occlusion or no-occlusion at that certain voxel. Because we only take into account static occlusion for the moment, we can run the occlusion detection once and use the results later on. In case of random camera combinations, we need to compute three visual hulls per camera per frame, hence 21 visual hulls (with seven cameras). This roughly results in 0.5 frames per second.

5.2 Classification

In Figure 6 we see the results of the algorithm.[1] The visited voxels have been classified into five classes: *occluded* (red), *non-occluded* (green), *undecided* (blue), *unknown* (gray) *and out of sight* (black). The voxels are classified by the votes t_{occluded}, t_{visible} and whether the voxel is visible by the camera:

[1]More results of the occlusion maps of these sequences can be found at
http://telin.ugent.be/~mslembro/?q=node/14

$$\text{Class} = \begin{cases} \text{occluded} & \text{if } t_{\text{occluded}} > t_{\text{visible}} \\ \text{non-occluded} & \text{if } t_{\text{occluded}} < t_{\text{visible}} \\ \text{undecided} & \text{if } t_{\text{occluded}} = t_{\text{visible}} \\ \text{unknown} & \text{if } t_{\text{occluded}} = t_{\text{visible}} = 0 \\ \text{out of sight} & \text{if voxel not in field of view} \end{cases} \tag{6}$$

Note that in the final occlusion map we assume *undecided* and *out of sight* as occluded and *unknown* as non-occluded and hence distinguish only two classes: occluded and non-occluded.

5.3 VISUAL HULL RESULTS

Using the generated occlusion maps we are now able to reconstruct a person, walking trough the room, without losing occluded parts. The occlusion maps of all cameras are evaluated to determine for each voxel separately which cameras are relevant to build the 3D model. Only cameras classified as *non-occluded* for a voxel are taken into account. In Figure 8 we see the visual hull constructed with and without occlusion mapping. The 3D model of the person is significantly more recognizable in Figure 8j which takes the occlusion into account.

6 CONCLUSION

In this paper we presented a self-learning occlusion map algorithm derived from the voxel perspective to improve the 3D reconstruction of an object in a scene with static occlusion. The method is based on the visual hull concept and builds a separate occlusion map for each camera. We designed a voting framework in order to classify voxels as occluded or non-occluded. We showed promising results from our test setup with seven cameras and one occluding object.

7 FUTURE WORK

As a first step we chose to only allow purely static occlusion. It is however also possible to have objects which are moved around in the scene e.g. chairs. The occlusion maps could be continuously updated in a parallel process. We could also estimate the shape of the occluding objects in the scene. If the camera positions and orientations are then changed. New occlusion maps could be automatically generated from the old ones without having to run the occlusion detection again.


(a)


(b)


(c)


(d)


(e)


(f)


(g)

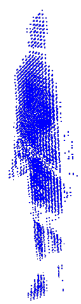
(h) Damaged 3D model due to ignoring occlusion

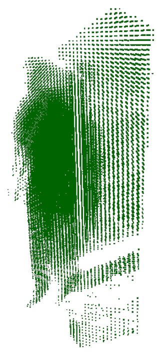
(i) State of the art

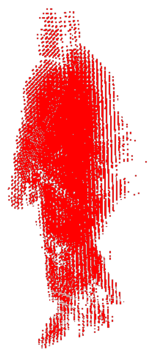
(j) Recognizable 3D model thanks to occlusion maps

Figure 8: a) - (g) Input images of all camera views. In (h) we ignore the occlusion information leading to an incorrect 3D shape. () shows the state of the art method where we see a lot of extra voxels which should not belong to the 3D model. In (j) on the other hand we still recognise a person in the 3D model because the cameras responsible for degrading the 3D shape are ignored.

REFERENCES

Apostoloff, N. and Fitzgibbon, A. (2005). Learning spatiotemporal t-junctions for occlusion detection. In *Computer Vision and Pattern Recognition, 2005. CVPR 2005. IEEE Computer Society Conference on*, volume 2, pages 553–559. IEEE.

Brostow, G. J. and Essa, I. A. (1999). Motion based decompositing of video. In *Computer Vision, 1999. The Proceedings of the Seventh IEEE International Conference on*, volume 1, pages 8–13. IEEE.

Corazza, S., Mündermann, L., Chaudhari, A., Demattio, T., Cobelli, C., and Andriacchi, T. (2006). A markerless motion capture system to study musculoskeletal biomechanics: Visual hull and simulated annealing approach. *Annals of Biomedical Engineering*, 34(6):1019–1029.

Corazza, S., Mündermann, L., Gambaretto, E., Ferrigno, G., and Andriacchi, T. P. (2010). Markerless motion capture through visual hull, articulated icp and subject specific model generation. *International journal of computer vision*, 87(1-2):156–169.

Favaro, P., Duci, A., Ma, Y., and Soatto, S. (2003). On exploiting occlusions in multiple-view geometry. In *Computer Vision, 2003. Proceedings. Ninth IEEE International Conference on*, pages 479–486. IEEE.

Grauman, K., Shakhnarovich, G., and Darrell, T. (2003). A bayesian approach to image-based visual hull reconstruction. In *Computer Vision and Pattern Recognition, 2003. Proceedings. 2003 IEEE Computer Society Conference on*, volume 1, pages I–187. IEEE.

Guan, L., Sinha, S., Franco, J.-S., and Pollefeys, M. (2006). Visual hull construction in the presence of partial occlusion. In *3D Data Processing, Visualization, and Transmission, Third International Symposium on*, pages 413–420. IEEE.

Kim, H., Sakamoto, R., Kitahara, I., Toriyama, T., and Kogure, K. (2006). Robust foreground segmentation from color video sequences using background subtraction with multiple thresholds. *Proc. KJPR*, pages 188–193.

Laurentini, A. (1994). The visual hull concept for silhouette-based image understanding. *Pattern Analysis and Machine Intelligence, IEEE Transactions on*, 16(2):150–162.

Zivkovic, Z. (2004). Improved adaptive gaussian mixture model for background subtraction. In *Pattern Recognition, 2004. ICPR 2004. Proceedings of the 17th International Conference on*, volume 2, pages 28–31 Vol.2.